

Abrikosov and the path to understanding high- T_c superconductivity

Juan Carlos Campuzano

Department of Physics, University of Illinois at Chicago, Chicago, Illinois 60607, USA

E-mail: jcc@uic.edu

Received January 5, 2018, published online April 25, 2018

An early attempt to try to understand the high superconducting transition temperatures in the cuprate superconductors was Abrikosov's theory of extended Van Hove singularities. It was based on our early experimental data on the $\text{YBa}_2\text{Cu}_3\text{O}_{6.9}$ and $\text{YBa}_2\text{Cu}_4\text{O}_8$ compounds which showed an extended saddle point singularity in the dispersion of the electronic excitations. This appeared to lead to a Van Hove singularity in the density of states with a divergence stronger than the known logarithmic one observed in conventional materials. The consequent high density of states of the extended singularity was thought to lead to high T_c 's in a conventional BCS mechanism. Unfortunately, it was soon realized that the very incoherent nature of the electronic excitations in these materials did not provide the expected high density of states. Here we summarize the many unusual characteristics of the electronic excitations in the cuprates, and what they imply for a possible theoretical description of high-temperature superconductivity.

PACS: 74.72.-h Cuprate superconductors;
74.25.Jb Electronic structure.

Keywords: cuprates, normal state, ARPES.

1. Introduction

When high-temperature superconductivity burst into the scene in 1986, many mechanisms were proposed to explain this remarkable phenomena, including the presence of a Van Hove singularity near the Fermi energy [1–4]. With this motivation, we examined the electronic structure in the two cuprate superconductors $\text{YBa}_2\text{Cu}_3\text{O}_{6.9}$ and $\text{YBa}_2\text{Cu}_4\text{O}_8$ by angle-resolved photoemission, and found an “extended” saddle point singularity in the energy spectrum in the neighborhood of the $(0, \pi)$ point [5]. This singularity occurs in the band derived from the CuO_2 planes at a binding energy of less than 30 meV [6].

Figure 1(a) shows the observed experimental band structure obtained along the $(0, 0) \rightarrow (0, 2\pi)$ symmetry line for the $\text{YBa}_2\text{Cu}_3\text{O}_{6.9}$ and $\text{YBa}_2\text{Cu}_4\text{O}_8$. It can be seen that a band disperses towards the Fermi energy, but does not cross it, remaining instead at a very small binding energy of ≈ 30 meV, as determined from the position of the highest intensity in the peak. The peak width is very narrow, being limited entirely by the instrumental resolution available at the time, again indicating that at these values of k_x, k_y , the band bottom is close to E_F , as shown in Fig. 1(b). We found that there is no observable

dispersion along k_z [7] for optimally doped samples, as shown in Fig. 2. This peak had been observed before by Manzke *et al.* [8] and Tobin *et al.* [9], although the nature of the singularity had not been appreciated [6]. A schematic representation of the experimental band structure is shown in Fig. 1(c).

2. Extended Van Hove model, and why it does not work

The experiment thus shows that is a saddle point singularity at the zone edge. The idea [5] was that the Van Hove singularity arising from such a saddle point increases the density of states, and therefore T_c . Van Hove singularities had been considered before (see, for example, Refs. 1–4), although the consequences of an extended singularity had not been considered. Another characteristic of the cuprate superconductors that needed to be accounted for was the suppression of the isotope effect, due to the fact that the integration limits in this case are determined not by the Debye frequency, but by the limits of the singularity, i.e., by some electronic energy scale. Even at the time of the publication of the Abrikosov paper [5], we pointed out that we were aware of the unusual nature of the normal state, which we intended to examine in a subsequent paper.

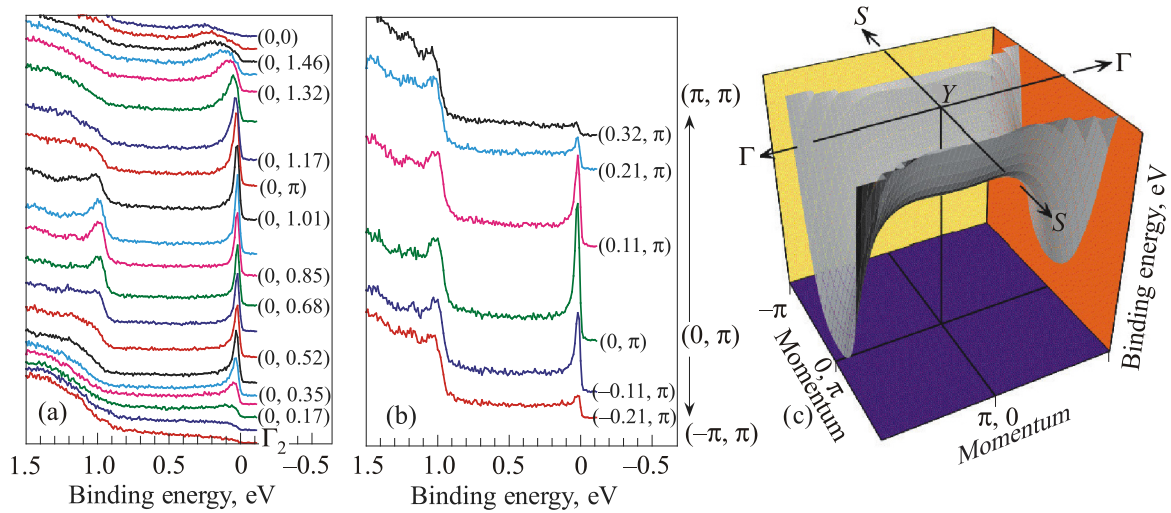


Fig. 1. (Color online) Dispersion of the single band important in the HTSC problem: (a) from the Brillouin zone center to the zone edge; (b) along the zone edge; and (c) a schematic representation of the dispersion.

However, that paper was not published. We later realized that the extended Van Hove singularity scenario did not in fact lead to a high T_c .

The reason for this, pictured in Fig. 3, is that the peaks near the Fermi energy are quite broad above T_c , of order 200 meV FWHM. The overlap of the particle and hole wavefunctions does not therefore lead to a high density of states. Here we find the first problem with the normal state of the cuprates, in that a BCS model cannot lead to superconductivity.

3. Properties of the normal state of the HTSCs

There are many other properties of the electronic excitations in the normal state of the cuprates which are most

unusual and difficult to understand. Moreover, there is no known path to a change in the nature of the electronic excitations going from the normal to the superconducting state. We will now summarize the properties of the elementary excitations of the normal state using symmetry-resolved photoemission (ARPES) data, obtained as follows [11]: The ARPES intensity $I(k, \omega)$ is proportional to $f(\omega)A(k, \omega)$, where A is the spectral function, and f is the Fermi function [10]. The effect of f can be eliminated from the ARPES data using the assumption of particle-hole symmetry $A(-\epsilon_k, -\omega) = A(\epsilon_k, \omega)$ for small $|\omega|$. Within the small k -window centered at k_F , one can show that the symmetrized intensity $I(\omega) + I(-\omega)$ at k_F is simply the

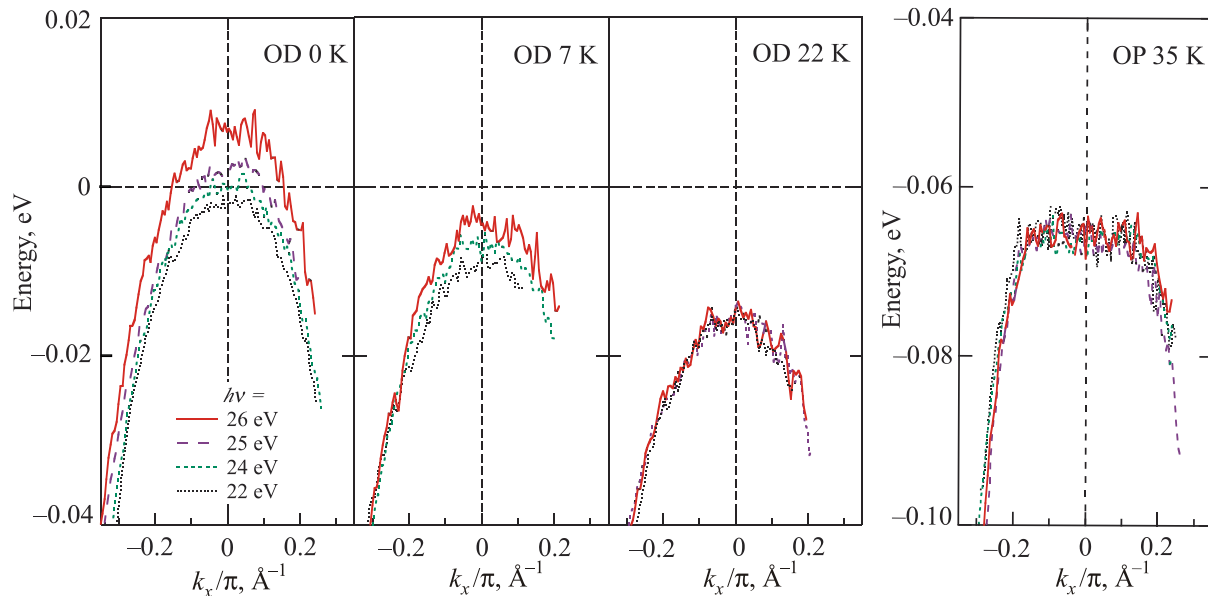


Fig. 2. (Color online) Dispersion along the direction perpendicular to the CuO_2 planes for $(\text{Bi,Pb})_2(\text{Sr,La})_2\text{CuO}_{6+\delta}$ samples vs. photon energy for the values of T_c 's indicated. The small dispersion of 10 meV along the k_z direction observed in an OD 0 K sample disappears with decreasing hole concentration. Note the very flat saddle point dispersion for the optimally doped sample. From Ref. 7.

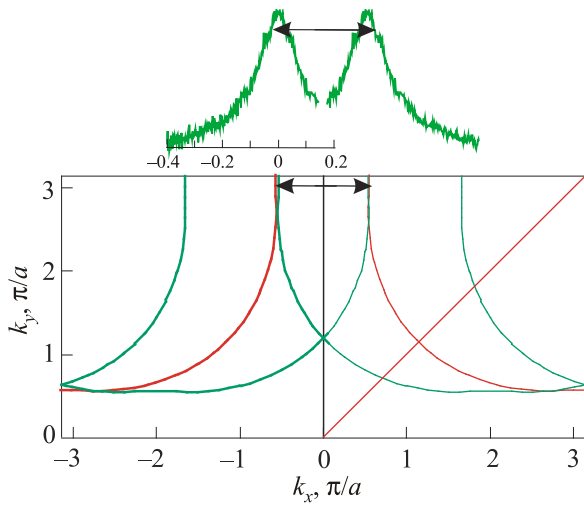


Fig. 3. (Color online) Effective umklapp is not favored by very incoherent excitations.

spectral function (convolved with the resolution). Results obtained from symmetrized data agree with those obtained from the leading edge of the raw data [11].

The varied and unusual properties of the electronic excitations around the phase diagram are summarized in Fig. 4

[13]. Figure 4(a) shows the temperature-doping phase diagram of BISCO. The points correspond to some of the data shown here. Unless stated otherwise, the data shown here were obtained at the antinode, where in the superconducting state the gap is maximum.

In Fig. 4(b) we show the electron spectral function in the region shaded pale red, dubbed the “strange metal” region, where the spectral function does not depend on temperature or doping. They can all be described by the same Lorentzian function, modulo an amplitude factor. This behavior is quite unusual, since normally doping strongly alters the charge screening radius, which in turn alters the lineshape. Since these spectra are much wider than temperature, perhaps it is not surprising neither doping nor temperature play a role in determining the lineshape. These facts lead us to think that the spectral functions do not correspond to usual quasi-particle excitations, but rather to collective excitations, whose nature still remains to be determined.

While the spectral function is invariant in the strange metal region, as the temperature is lowered, it evolves into spectral functions of quite different nature at different doping values. For example, the excitations which are to the left of optimal doping acquire a “pseudogap” at a crossover temperature T^* , as shown in Fig. 4(b) [12]. The pseudogap

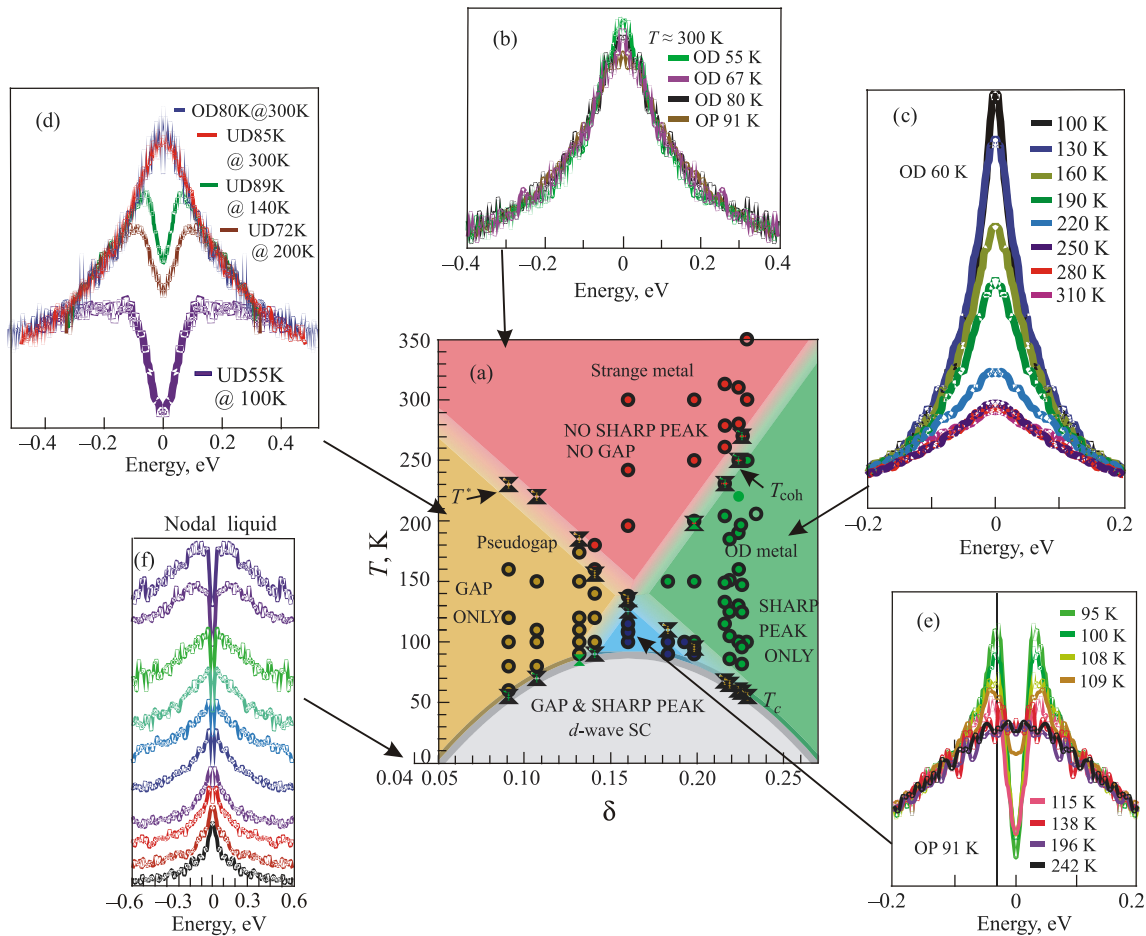


Fig. 4. (Color online) Electronic excitation spectra at the point of maximum gap along the Fermi surface.

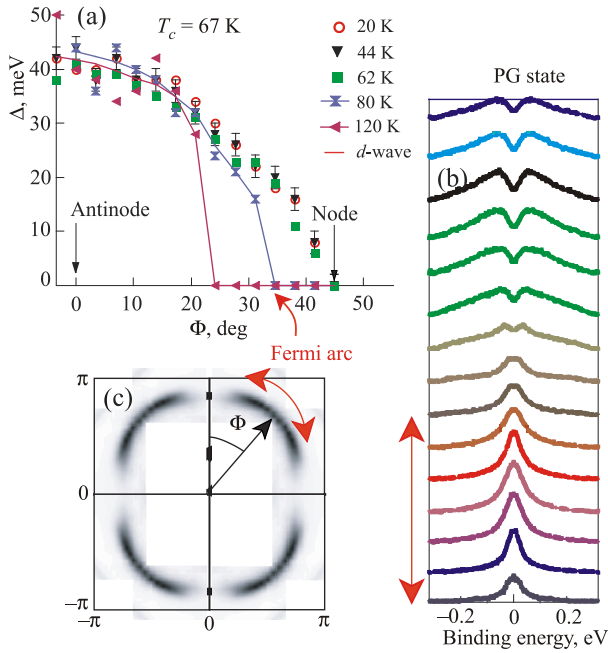


Fig. 5. (Color online) Electronic excitations around the Fermi surface. (a) Relative value of the pseudogap as a function of angle along the Fermi surface, schematically shown in (c). (b) Spectra showing portions of the Fermi surface which are pseudogapped and portions which have a Fermi arc, indicated by the red arrow. (c) Plot of the spectral intensity at the chemical potential along the Fermi surface, showing the regions which are gapped, and those which form the Fermi arcs.

becomes more pronounced as either the doping decreases or the temperature is lowered. Once the superconducting phase transition takes place, the pseudogap turns into the superconducting gap at T_c .

On the other hand, strange metal excitations on the right of optimal doping evolve into Fermi-liquid quasiparticle excitations at a temperature T_{coh} , as shown in Fig. 4(c). Not surprisingly, the onset of Fermi-liquid behavior occurs at progressively higher coherence temperatures as the doping increases and charge screening also increases.

What is not expected however, is that the T^* and T_{coh} lines cross, defining a region of the phase diagram where the pseudogap and coherent excitations coexist, as exemplified by the spectra shown in Fig. 4(e). Sharp peaks corresponding to coherent excitations appear at the edges of the pseudogap. The crossing of the T^* and T_{coh} lines is unlike many sketches in the literature, where the two lines do not cross. Also, in our phase diagram the T^* line is tangent to the T_c dome.

An additional property of the pseudogap is that at its onset, it exists over a region of the Fermi surface near the antinodes of the superconducting gap, as shown in Fig. 5 [15,14]. The rest of the Fermi surface forms arcs, unexpected because in metals, the Fermi surface is continuous. These arcs contract as the temperature is lowered, and turn

into the point nodes of the superconducting state (Fig. 5(a)). The Fermi arcs scale, becoming smaller as the doping decreases [15].

Once the doping is sufficiently low, such that $T_c = 0$, the material becomes a nodal metal [16], a most unusual state, where the entire Fermi surface is gapped, except for the four protected point nodes, as shown in Fig. 4(f).

From the brief descriptions of the excitations in the normal state of the cuprate superconductors, it is clear that the formulation of a theory that accounts for all the amazing phenomena described above will be a monumental task.

The work summarized here could not have possibly come to fruition without each one of the experimental collaborators over nearly three decades, each having played crucial roles in the study of the cuprate superconductors. However, I would like to particularly thank theoreticians Alexei Abrikosov, Mohit Randeria and Michael Norman, who had the most impact in helping us experimentalists understand the significance of our results.

1. J.E. Hirsh and D.J. Scalapino, *Phys. Rev. Lett.* **56**, 2735 (1986).
2. J. Friedel, *J. Phys.: Condens. Matter* **1**, 7757 (1989).
3. R.S. Markiewicz, *Int. J. Mod. Phys. B* **5**, 2037 (1991); R.S. Markiewicz and B.G. Giessen, *Physica C* **160**, 497 (1989); R.S. Markiewicz, *J. Phys.: Condens. Matter* **2**, 665 (1990) and references therein; L. Van Hove, *Phys. Rev.* **89**, 1189 (1953).
4. D.M. Newns, H.R. Krishnamurphy, P.C. Pattnaik, C.C. Tsuei, and C.L. Kane, *Phys. Rev. Lett.* **69**, 1264 (1992); D.M. Newns, P.C. Pattnaik, and C.C. Tsuei, *Phys. Rev. B* **43**, 3075 (1991).
5. A.A. Abrikosov, J.C. Campuzano, and K. Gofron, *Physica C* **214**, 73 (1993).
6. K. Gofron, J.C. Campuzano, H. Ding, D. Koelling, A.A. Abrikosov, A. Bansil, M. Lindroos, and B. Dabrowski, *Phys. Rev. Lett.* **73**, 3302 (1994).
7. T. Takeuchi, T. Kondo, T. Kitao, H. Kaga, H. Yang, H. Ding, A. Kaminski, and J.C. Campuzano, *Phys. Rev. Lett.* **95**, 227004 (2005).
8. R. Manzke, G. Mante, R. Claessen, M. Skibowski, and J. Fink, *Surf. Sci.* **269**, 1066 (1992) and references therein.
9. J.G. Tobin, C.G. Olson, C. Gu, J.Z. Liu, F.R. Solal, M.J. Russ, R.H. Howell, J.C. O'Brien, H.B. Radousky, and P.A. Sterne, *Phys. Rev. B* **45**, 5563 (1992).
10. M. Randeria, H. Ding, J.C. Campuzano, A.F. Bellman, G. Jennings, T. Yokoya, T. Takahashi, H. Katayama-Yoshida, T. Mochiku, and K. Kadowaki, *Phys. Rev. Lett.* **74**, 4951 (1995).
11. M.R. Norman, M. Randeria, H. Ding, and J.C. Campuzano, *Phys. Rev. B* **97**, R11093 (1998).
12. H. Ding, T. Yokoya, J.C. Campuzano, T. Takahashi, M. Randeria, M.R. Norman, T. Mochiku, K. Kadowaki, and J. Giapintzakis, *Nature* **382**, 51 (1996).

13. U. Chatterjee, D. Ai, J. Zhao, S. Rosenkranz, A. Kaminski, H. Raffy, Z. Li, K. Kadowaki, M. Randeria, M.R. Norman, and J.C. Campuzano, *Proc. Nat. Acad. Sci.* **108**, 9346 (2011).
 14. A. Kanigel, M.R. Norman, M. Randeria, U. Chatterjee, S. Souma, A. Kaminski, H.M. Fretwell, S. Rosenkranz, M. Shi, T. Sato, T. Takahashi, Z.Z. Li, H. Raffy, K. Kadowaki, D. Hinks, L. Ozyuzer, and J.C. Campuzano, *Nat. Phys.* **2**, 447 (2006).
 15. A. Kanigel, U. Chatterjee, M. Randeria, M.R. Norman, S. Souma, M. Shi, Z.Z. Li, H. Raffy, and J.C. Campuzano, *Phys. Rev. Lett.* **99** 157001 (2007).
 16. U. Chatterjee, M. Shi, D. Ai, J. Zhao, A. Kanigel, S. Rosenkranz, H. Raffy, Z.Z. Li, K. Kadowaki, D.G. Hinks, Z.J. Xu, J.S. Wen, G. Gu, C.T. Lin, H. Claus, M.R. Norman, M. Randeria, and J.C. Campuzano, *Nature Phys.* **6**, 99 (2009).
-